THE JOURNAL OF BIOLOGICAL CHEMISTRY VOL. 287, NO. 51, pp. 42951–42961, December 14, 2012

Peroxisome Proliferator-activated Receptor-γ Activation Enhances Insulin-stimulated Glucose Disposal by Reducing *ped/pea-15* Gene Expression in Skeletal Muscle Cells

EVIDENCE FOR INVOLVEMENT OF ACTIVATOR PROTEIN-1[*]

Received for publication, July 31, 2012, and in revised form, October, 25, 2012 Published, JBC Papers in Press, October 26, 2012, DOI 10.1074/jbc.M112.406637

Paola Ungaro[‡1,2], **Paola Mirra**[‡1], **Francesco Oriente**[§], **Cecilia Nigro**[‡], **Marco Ciccarelli**[§], **Viviana Vastolo**[‡§], **Michele Longo**[‡], **Giuseppe Perruolo**[‡], **Rosa Spinelli**[§], **Pietro Formisano**[§], **Claudia Miele**[‡], **and Francesco Beguinot**[‡§]

From the [§]*Dipartimento di Biologia e Patologia Cellulare e Molecolare, Università di Napoli "Federico II" and the* [‡]*Istituto di Endocrinologia e Oncologia Sperimentale Gaetano Salvatore, Consiglio Nazionale delle Ricerche, 80131 Naples, Italy*

Background: PPARγ modulation of glucoregulatory response in skeletal muscle has been only partially elucidated.
Results: PPARγ inhibits the transcription of the diabetes-associated gene *ped/pea-15* via AP-1.
Conclusion: *ped/pea-15* is downstream of a PPARγ-regulated inflammatory network.
Significance: These studies further elucidate the gene network responsible for inflammation-induced insulin resistance.

The gene network responsible for inflammation-induced insulin resistance remains enigmatic. In this study, we show that, in L6 cells, rosiglitazone- as well as pioglitazone-dependent activation of peroxisome proliferator-activated receptor-γ (PPARγ) represses transcription of the *ped/pea-15* gene, whose increased activity impairs glucose tolerance in mice and humans. Rosiglitazone enhanced insulin-induced glucose uptake in L6 cells expressing the endogenous *ped/pea-15* gene but not in cells expressing *ped/pea-15* under the control of an exogenous promoter. The ability of PPARγ to affect *ped/pea-15* expression was also lost in cells and in C57BL/6J transgenic mice expressing *ped/pea-15* under the control of an exogenous promoter, suggesting that *ped/pea-15* repression may contribute to rosiglitazone action on glucose disposal. Indeed, high fat diet mice showed insulin resistance and increased *ped/pea-15* levels, although these effects were reduced by rosiglitazone treatment. Both supershift and ChIP assays revealed the presence of the AP-1 component c-JUN at the *PED/PEA-15* promoter upon 12-*O*-tetradecanoylphorbol-13-acetate stimulation of the cells. In these experiments, rosiglitazone treatment reduced c-JUN presence at the *PED/PEA-15* promoter. This effect was not associated with a decrease in c-JUN expression. In addition, c-*jun* silencing in L6 cells lowered *ped/pea-15* expression and caused nonresponsiveness to rosiglitazone, although c-*jun* overexpression enhanced the binding to the *ped/pea-15* promoter and blocked the rosiglitazone effect. These results indicate that PPARγ regulates *ped/pea-15* transcription by inhibiting c-JUN binding at the *ped/pea-15* promoter. Thus, *ped/pea-15* is downstream of a major PPARγ-regulated inflammatory network. Repression of *ped/pea-15* transcription might contribute to the PPARγ regulation of muscle sensitivity to insulin.

Peroxisome proliferator-activated receptor-γ (PPARγ)[3] is a member of the nuclear hormone receptor superfamily. In addition to other PPAR isoforms, this superfamily also includes the receptors for thyroid hormones, retinoids, steroid hormones, and vitamin D (1, 2). PPARγ regulates gene transcription by binding with the retinoid X receptors to specific DNA sequences termed peroxisome proliferator response elements (3). After ligand activation, PPARγ modifies its conformation, which facilitates the release of corepressors and subsequent binding of a distinct set of nuclear coactivators, thereby fostering PPARγ action (3). Ultimately, formation of these transcriptional complexes enables PPARγ transcriptional control of a variety of biological processes, including insulin sensitivity (4). Indeed, PPARγ exerts important modulatory actions upstream of the major inflammatory networks involving AP-1 and NF-κB transcriptional regulation (5).

PPARγ activation by thiazolidinediones (TZDs) markedly improves insulin sensitivity in type 2 diabetic patients (6–9). However, the molecular mechanisms responsible for PPARγ-mediated insulin sensitization have been only partially defined. Studies in tissue-specific PPARγ knock-out mice have generated insight into the role of different tissues in PPARγ-mediated regulation of systemic insulin-stimulated glucose metabolism (10) (2, 11). To date, the relevance of PPARγ in maintaining systemic insulin sensitivity in adipose tissues has been convincingly demonstrated. In fact, the PPARγ-mediated adipogenesis associated with the capability for fatty acid trapping has emerged as a major factor in protecting against non-adipose tissue insulin resistance (12). Skeletal muscle expression of PPARγ has further been shown to contribute to systemic insulin sensitivity by maintaining intact insulin-mediated glucose utilization in muscle (10). Indeed, PPARγ was reported to directly coordinate glucoregulatory responses in this tissue (11). However, the genetic network responsible for

* This study was supported in part by European Community FP6 PREPOBEDIA Grant 201681, the European Foundation for the Study of Diabetes, the Associazione Italiana per la Ricerca sul Cancro, and by Ministero dell'Università e della Ricerca Scientifica Grants PRIN and FIRB-MERIT.
[1] Both authors contributed equally to this work.
[2] To whom correspondence should be addressed. E-mail: pungaro@ieos.cnr.it.

[3] The abbreviations used are: PPARγ, peroxisome proliferator-activated receptor-γ; TZD, thiazolidinedione; Ptz, pioglitazone; TPA, 12-*O*-tetradecanoylphorbol-13-acetate; qRT-PCR, quantitative RT-PCR; Rtz, rosiglitazone; CRE, cAMP-response element.

these functions in skeletal muscle has not been completely elucidated yet.

Phosphoprotein Enriched in Diabetes/Phosphoprotein Enriched in Astrocytes (PED/PEA-15) is a scaffold cytosolic protein widely expressed in most human tissues (13, 14). Early studies indicated that PED/PEA-15 has an important role in controlling glucose disposal in the skeletal muscle by impacting on the phospholipase D/protein kinase C signaling network (15, 16). Further investigations demonstrated that PED/PEA-15 is commonly overproduced in individuals with type 2 diabetes as well as in their euglycemic offspring, causing skeletal muscle insulin resistance in these individuals (17). PED/PEA-15 cellular levels are regulated by ubiquitinylation and proteosomal degradation (18). In addition, run-on experiments in cultured cells from type 2 diabetic patients have demonstrated that PED/PEA-15 overproduction is caused, at least in part, by transcriptional abnormalities (13). More recent studies evidenced that epigenetic changes at the *PED/PEA-15* gene have a major role in controlling its transcription (19). However, the molecular details responsible for regulation of *PED/PEA-15* transcription as well as the abnormalities in these mechanisms occurring in type 2 diabetes remain unclear.

In this report, we demonstrate that PPARγ represses the transcription of the diabetes-associated gene *ped/pea-15*. We found that PPARγ repression of this gene requires displacement of the c-JUN component of the AP-1 transcriptional complex from the *ped/pea-15* promoter. These findings identify *ped/pea-15* as a gene downstream of major PPARγ-regulated inflammatory networks, whose control may be instrumental to PPARγ action on glucose disposal by the skeletal muscle.

EXPERIMENTAL PROCEDURES

Materials—Rosiglitazone and pioglitazone (Ptz) were purchased from Cayman Chemical (Ann Arbor, MI). 12-*O*-Tetradecanoylphorbol-13-acetate (TPA) and GW9662 were purchased from Sigma. Solutions were prepared in dimethyl sulfoxide (DMSO) and diluted 1:1000 into serum-free DMEM immediately before use. PPARγ, c-JUN, and 14-3-3ϵ antibodies were purchased from Santa Cruz Biotechnology (Santa Cruz, CA), and the PED/PEA-15 antibody was purchased from Cell Signaling Technology (Danvers, MA). Oligonucleotides, including the scrambled phosphorothioate oligodeoxynucleotide and the rat c-Jun antisense (20), were synthesized by Sigma. [γ-^{32}P]dATP and 2-[1-^{14}C]deoxy-D-glucose, were purchased from PerkinElmer Life Sciences. The pPED2000-Luc and pPED210-Luc constructs have been previously described (21). Site-directed mutagenesis of the CRE-like site was achieved using the QuikChange site-directed mutagenesis kit according to the manufacturer's instructions (Stratagene, La Jolla, CA). The following oligonucleotides were validated by EMSA and used to create the desired mutation: CREmut.F 5′-CCGGCTCTGACATTGCCGGCCAGCCGGG-3′ and CREmut.R 5′-CCCGGCTGGCCGGCAATGTCAGAGCCGG-3′. Mutant clones were screened by DNA sequencing. The pcDNA3 expression vector containing the Myc-tagged PED/PEA-15 has also been reported previously (22). The (PPRE)3-tk-luciferase construct (23) was donated by Dr. Mitchell Lazar (University of Pennsylvania). The dominant negative PPARγ expression vector, the L468A/E471A h-PPARγ double mutant (24), was donated by V. Krishna K. Chatterjee from University of Cambridge, United Kingdom. The expression vector (pCEFL) for c-Jun-HA was provided by Dr. Musti (University of Cosenza, Italy).

Cell Culture Studies—L6 skeletal muscle cells and HeLa cells were cultured in Dulbecco's modified Eagle's medium (DMEM) supplemented with 10% fetal bovine serum (FBS) and 1% penicillin/streptomycin solution at 37 °C in a humidified 95% air and 5% CO_2 atmosphere. L6 myoblasts were plated at a density of 3×10^4 cells/ml, and differentiation of confluent cells was initiated by reducing the FBS content of the media to 2% with a medium change every 48 h. Differentiation of myoblasts into multinucleated myotubes was completed by 7 days after medium change. Fused multinucleated myotubes were incubated with the serum-depleted (0.5%) medium for 16 h and treated with TZDs at the indicated concentrations for a further 24 h, although control cells received the vehicle alone in the serum-depleted (0.5%) medium. L6 myoblasts were electroporated with the Neon Transfection System (Invitrogen), and L6 myotubes and HeLa cells were transfected using Lipofectamine 2000 (Invitrogen), according to the manufacturer's instructions (15). All cell culture media and reagents were from Lonza (Basel, Switzerland).

Glucose uptake in L6 cells was assayed as reported previously (25). Briefly, the cells were incubated for 24 h in serum-free medium supplemented with 0.25% (w/v) bovine serum albumin (BSA) in the absence or presence of 1 μM Rtz. The cells were rinsed in glucose-free HEPES buffer (5 mM KCl, 120 mM NaCl, 1.2 mM $MgSO_4$, 10 mM $NaHCO_3$, 1.2 mM $KHPO_4$, and 20 mM HEPES, pH 7.8, 2% albumin) and further exposed to 100 nM insulin for 30 min. 2-Deoxy-D-[^{14}C]glucose uptake was measured over a 10-min period, with nonspecific uptake determined in the presence of cytochalasin-B.

Animal Studies—5-Week-old male C57BL/6J mice were hosted at the common facility of the University of Naples Medical School and had free access to water and food. For high fat diet treatment, mice were fed a high fat diet with ~60 cal % fat or a standard diet with ~10 cal % fat (Research Diets, New Brunswick, NJ) (26) for 12 weeks. During the last 10 days, the animals received either 10 mg/kg/die Rtz or vehicle alone (0.5% carboxymethylcellulose) by oral gavage. For insulin tolerance testing, mice were fasted for 4 h and then subjected to intraperitoneal injection with insulin (0.75 milliunits g^{-1} of body weight). Venous blood was subsequently drawn by tail clipping at 0, 15, 30, 45, 60, 90, and 120 min as in Ref. 27. For intraperitoneal glucose tolerance testing, mice were fasted overnight and then subjected to intraperitoneal injection with glucose (2.0 g kg^{-1} of body weight). Venous blood was subsequently drawn by tail clipping at 0, 15, 30, 45, 60, 90, and 120 min as in Ref. 27. In overnight fasted mice, serum insulin concentrations were measured by rat insulin RIA kit (Millipore, Billerica, MA) (27). Blood glucose levels were measured with Accu-Chek® glucometers (Roche Applied Science). In overnight fasted mice, analyses of serum triglycerides, total cholesterol, HDL cholesterol, and LDL cholesterol were done on Horiba ABX Pentra 400 Chemistry Analyzer (HORIBA ABX, Montpellier, France). The animals were sacrificed, and skeletal muscle tissues (gas-

trocnemius) were removed, rinsed with 0.9% NaCl, frozen in liquid nitrogen, and kept in −80 °C before harvesting.

Western Blot Analysis—Cells were solubilized by scraping and passed 10 times through a 25-gauge needle in ice-cold lysis buffer, supplemented with the Complete Protease Inhibitor Mixture Tablets (Roche Applied Science). Lysates were clarified by centrifugation at 16,000 × *g* for 10 min at 4 °C, and protein concentration was determined using the protein assay based on Bradford's method (Bio-Rad) (28). Total cell extracts in equal amounts were separated by SDS-PAGE and blotted on nitrocellulose membranes (Millipore, Billerica, MA). Membranes were blocked in 5% BSA, and specific proteins were detected by incubation with appropriate primary and secondary antibodies (horseradish peroxidase-conjugated) in 150 mM NaCl, 50 mM Tris, 0.5% Tween 20 (TBST). Protein bands were visualized using an enhanced chemiluminescence (ECL) kit (Thermo Scientific Pierce Protein Biology, Waltham, MA) and quantified by the ImageJ software (a public domain and Java-based image processing program developed at the National Institutes of Health). Relative protein abundance was calculated after 14-3-3ϵ normalization.

Real Time PCR Analysis—Total RNA was extracted with the TRIzol reagent (Invitrogen), according to the manufacturer's protocol. Reverse transcription of 1 μg of total RNA was performed using SuperScript III (Invitrogen), following the manufacturer's instructions. Quantitative real time PCR was performed in triplicate by using iQ SYBR Green Supermix on iCycler real time detection system (Bio-Rad). Relative quantification of gene expression was calculated by the ΔΔ*Ct* method (29). Each *Ct* value was first normalized to the respective glyceraldehyde-3-phosphate dehydrogenase (GAPDH) *Ct* value of a sample to account for variability in the concentration of RNA and in the conversion efficiency of the RT reaction. For copy number analysis, the real time PCR amplification products for *ped/pea-15* and *gapdh* were cloned into the pGEM®-T easy vector (Promega, Madison, WI), and calibration curves were made from serial 10-fold dilutions of plasmid DNAs as described previously (30). The mean slopes of the calibration curves for the two genes were similar, −3.3 for *ped/pea-15* and −3.1 for *gapdh*, where a slope of −3.3 ± 10% reflects an efficiency of 100 ± 10% of the PCR r, and the mean correlation coefficient (*R*) for both of the curves was 0.99. The equations drawn from the graph of the standard curves were used to calculate the precise number of specific cDNA molecules present in the samples (copy number variation).

Luciferase Assays—Cells were cotransfected with 2 μg of the Firefly luciferase vector (pGL3 plasmids, Promega, Madison, WI) and 1 μg of the pRSV-β-galactosidase (Promega, Madison, WI), as internal control to normalize for transfection efficiency. In each reaction, the total amount of transfected DNA was kept constant at 5 μg by using the empty expression vector pcDNA3 or PPARγ$_{L468A/E471A}$ mutant. 24 h after transfection, cells were incubated with the serum-depleted (0.5%) medium for 16 h and then exposed to serum-depleted (0.5%) medium supplemented with vehicle (0.1% DMSO) or TPA (0.1 μM) in the absence or presence of increasing concentrations of Rtz for 4 h. Luciferase and β-galactosidase activities were measured with a luminometer (Berthold Technologies, Bad Wildbad, Germany). Luciferase activities were divided by the respective β-galactosidase activity and expressed as relative luciferase units.

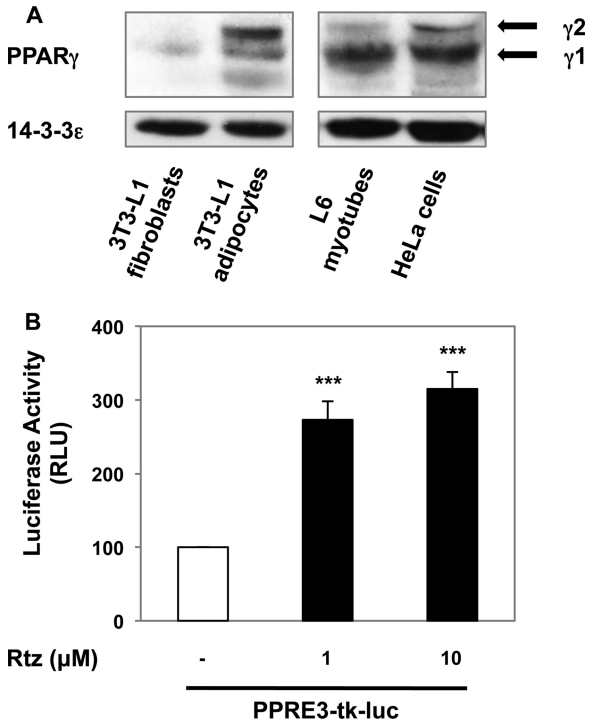

FIGURE 1. **PPARγ expression and function in L6 skeletal muscle cells.** *A*, 3T3-L1 fibroblasts, 3T3-L1 adipocytes, L6 myotubes, and HeLa cells were lysed, and total protein extracts were separated by SDS-PAGE. The antibodies used were specific for PPARγ and 14-3-3ϵ as loading control. The autoradiograph shown is representative of four additional experiments. *B*, L6 myotubes were cotransfected with PPRE3-tk-luc and pRSV-β-gal constructs as described under "Experimental Procedures." Upon transfection, the cells were incubated in the absence or presence of the indicated concentrations of Rtz. Luciferase and β-galactosidase activities were measured in cellular extracts 24 h later. β-Galactosidase activity enabled the estimation of transfection efficiency and assessment of relative luciferase values (*RLU*). *Bars* represent the means ± S.D. of three independent experiments. *Asterisks* indicate statistically significant differences at a $p < 0.001$ level.

Electrophoretic Mobility Gel Shift (EMSA) and Supershift Assays—Nuclear extracts from HeLa cells were prepared as described previously with minor modifications (31). Double-stranded oligonucleotides were end-labeled with [γ-^{32}P]ATP by T4 polynucleotide kinase (Promega, Madison, WI) according to the manufacturer's instructions. The radiolabeled probes were purified by spin columns (Roche Applied Science). 5 μg of nuclear protein extracts from control and treated cells were incubated with 100,000 cpm ^{32}P-labeled oligonucleotide probe in 25 mM HEPES, pH 7.4, 50 mM KCl, 10% glycerol (v/v), 5 mM dithiothreitol (DTT), and 1 μg of poly(dI-dC) (GE Healthcare) for 30 min at room temperature in a final volume of 20 μl. Upon binding, protein-DNA complexes were separated on 6% non-denaturing polyacrylamide gels at 120 V in 0.5× TBE buffer. Gels were dried and further subjected to PhosphorImager analysis (Bio-Rad). In competition analysis, 25-, 50-, and 100-fold molar excess of the unlabeled double strand oligonucleotide was added to the reaction mixture prior to the addition of the labeled probe. For the antibody supershift analysis, 1 μg of antibody was added to the nuclear extracts prior to the radiolabeled oligonucleotide.

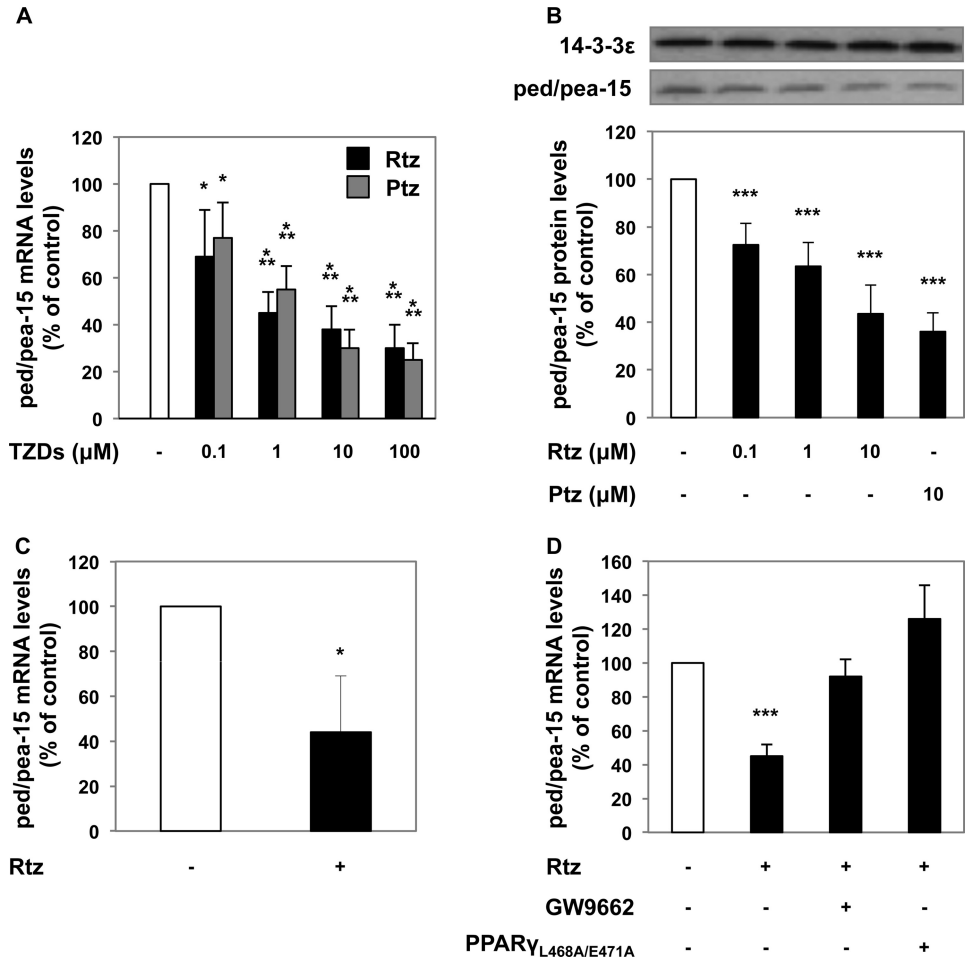

FIGURE 2. **PPARγ repression of *ped/pea-15* transcription.** *A,* L6 myotubes were incubated in the presence of the indicated concentrations of Rtz (*black bars*) or Ptz (*gray bars*) for 24 h. Total RNA was obtained, and *ped/pea-15* and *gapdh* mRNA levels were measured by qRT-PCR. Values were normalized for *gapdh* and presented as fold decrease relative to the control (untransfected cells). *B,* L6 myotubes were incubated in the absence or presence of Rtz for 24 h. Total protein extracts were separated by SDS-PAGE followed by immunoblotting with PED/PEA-15 or 14-3-3ϵ antibody, as indicated. The one presented is representative of two additional experiments with very similar results. *C,* total RNA was obtained from gastrocnemius of C57BL/6J mice treated or not with 10 mg/kg/die Rtz for 10 days. The mRNAs were assessed by qRT-PCR. *ped/pea-15* values were normalized for *gapdh* and expressed as fold decrease *versus* control. *D,* L6 myotubes were preincubated with 10 μM GW9662 for 1 h or transfected with the $PPAR\gamma_{L468A/E471A}$ mutant as described under "Experimental Procedures" and then treated with 1 μM Rtz for 24 h. Total RNA was obtained, and *ped/pea-15* and *gapdh* mRNA levels were measured by qRT-PCR. Values were normalized for *gapdh* and presented as fold decrease relative to the control. *Bars* represent the means ± S.D. of three (*A* and *D*) and four independent experiments (*B*). Five mice/group were used in *C*. *Asterisks* denote statistically significant differences (*, $p < 0.05$; **, $p < 0.01$, and ***, $p < 0.001$).

Chromatin Immunoprecipitation Assay (ChIP)—ChIP assays were performed as reported previously (21). Briefly, upon protein-DNA cross-linking, cells were lysed and sonicated to achieve chromatin fragments ranging between 500 and 1000 bp in size. The lysates were incubated with either c-JUN antibody or a rabbit control IgG, and then complexes were isolated using protein A-agarose/salmon sperm DNA (Millipore, Billerica, MA). Immunoprecipitates were extensively washed and then eluted by freshly prepared 1% SDS, 0.1 M $NaHCO_3$ buffer. After reversion of cross-linking, DNA was purified by the QIAquick PCR purification kit (Qiagen, Hilden, Germany) followed by PCR amplification. PCR products were resolved by 2% agarose gel electrophoresis, revealed by ethidium bromide staining, and analyzed by densitometry using the ImageJ software (National Institutes of Health).

Statistical Analysis—All data are presented as means ± S.E. Statistical differences were determined by one- or two-way analysis of variance as appropriate, and Bonferroni post hoc testing was performed when applicable. A p value <0.05 was considered significant.

RESULTS

PPARγ Regulates ped/pea-15 Function in Muscle Cells—We assessed PPARγ expression in the L6 skeletal muscle cell line by Western blot analysis. The PPAR-specific antibody detected both the isoforms 1 and 2, which have a predicted molecular mass of ~53 and 57 kDa, respectively. In L6 myotubes as well as in HeLa cells, the γ1 isoform was more abundant than the γ2 isoform, although PPARγ2 was the most highly expressed isoform in 3T3-L1 adipocytes. At variance, 3T3-L1 fibroblasts showed very low PPARγ levels (Fig. 1*A*). L6 cells were also transfected with a construct featuring the PPAR response element upstream from the luciferase gene (PPRE3-tk-luc). As shown in Fig. 1*B*, treatment of these cells with increasing amounts of the PPARγ agonist Rtz determined a significant

increase in the promoter activity, indicating that PPARγ is transcriptionally active in L6 cells.

PPARγ has been reported to regulate a number of genes controlling metabolic functions (32). Interestingly, in L6 myotubes, Rtz and Ptz repressed *ped/pea-15* expression in a dose-dependent manner, and this effect occurred both at mRNA (Fig. 2*A*) and at protein levels (Fig. 2*B*). A comparable decrease in *ped/pea-15* mRNA levels was also observed in the skeletal muscle of Rtz-treated C57BL/6J mice (Fig. 2*C*). In addition, both pretreatment of L6 cells with the PPARγ antagonist GW9662 and transfection with the dominant negative PPARγ mutant, $PPAR\gamma_{L468A/E471A}$, completely abolished the Rtz effect (Fig. 2*D*), indicating that TZDs inhibit *ped/pea-15* expression via PPARγ.

The known physiological importance of PED/PEA-15 in regulating glucose tolerance prompted us to further investigate the molecular details of the TZDs action on ped/pea-15 function. To this end, we transfected L6 cells with a *myc*-tagged *PED/PEA-15* cDNA driving the expression of the gene under the control of the cytomegalovirus (CMV) promoter, and then we exposed the cells to Rtz. As shown in Fig. 3*A*, Rtz did not affect the levels of the exogenous PED/PEA-15 protein (21 kDa), although it reduced the levels of the endogenous one (15 kDa). Consistent with these findings, treatment with Rtz did not significantly affect PED/PEA-15 protein levels in the skeletal muscle of transgenic mice overexpressing this gene under the control of the exogenous β-actin promoter (Tg_{ped}), although it reduced endogenous PED/PEA-15 protein levels up to 60% in their wild-type littermates (Fig. 3*B*). Furthermore, as shown in Fig. 3*C*, Rtz enhanced glucose uptake in wild-type L6 cells ($L6_{WT}$) but not in those cells expressing the exogenous PED/PEA-15 ($L6_{ped}$). Thus, it appeared that the endogenous *ped/pea-15* promoter is necessary for PPARγ regulation of the gene.

PPARγ Silences ped/pea-15 by Interfering with AP-1 Signaling—These findings led us to explore the molecular mechanisms involved in PPARγ regulation of *ped/pea-15* in greater detail and to identify the PPARγ responding region at the *ped/pea-15* promoter. Previous studies in cells treated with TPA, a known activator of both AP-1 and NF-κB, revealed increased *PED/PEA-15* expression (18). We have therefore addressed the hypothesis that PPARγ reduces *PED/PEA-15* transcription by transrepressing one or both of these transcription factors. *In silico* analysis of the human *PED/PEA-15* promoter revealed the presence of a TGACATCA CRE-like site between the positions −106 and −86 bp from the transcription start site (+1). This sequence is known to bind the AP-1 transcriptional complex (33). A caGGGActtt NF-κB-binding site between positions −798 and −786 bp was also identified. Furthermore, sequence alignment of the human and rat 5′-flanking regions revealed that these two sequences are highly conserved, suggesting they may perform a major role in regulating *PED/PEA-15* expression and prompted us to test the significance of AP-1 and NF-κB in the PPARγ-dependent regulation of the *PED/PEA-15* promoter.

To this goal, we transfected HeLa cells with a reporter vector featuring the *luciferase* gene downstream from the −1942 to +58 bp of the proximal 5′-flanking region of the human *PED/PEA-15* gene (pPED2000). In these transfected cells, TPA up-

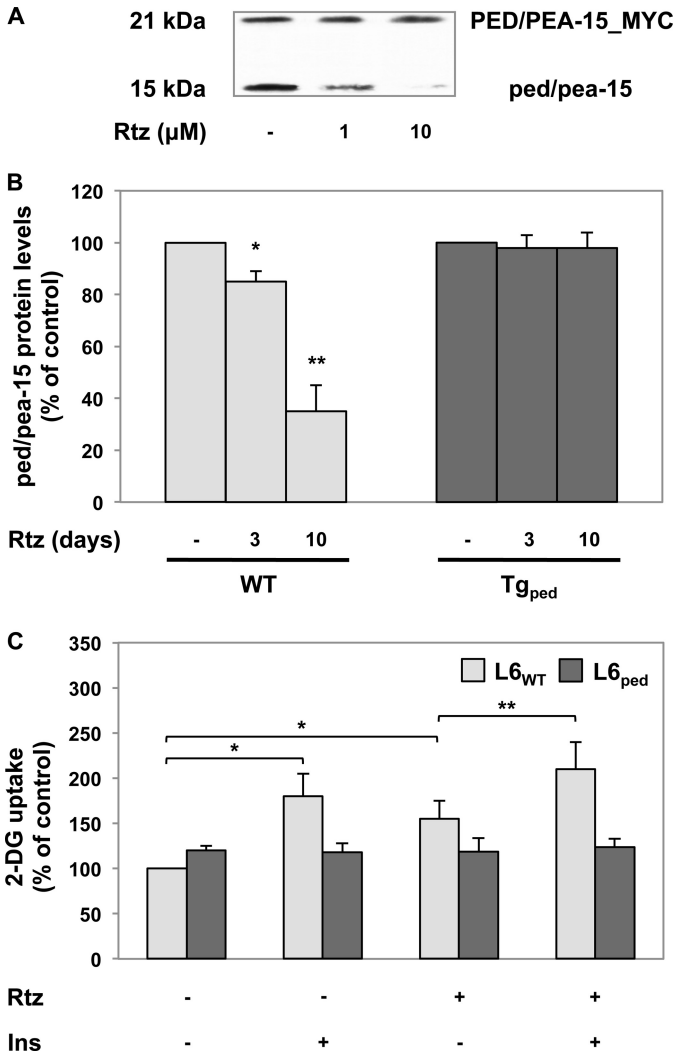

FIGURE 3. **Significance of *ped/pea-15* promoter to PPARγ-dependent repression.** *A*, L6 myotubes were transfected with a pcDNA3 expression vector containing a Myc-tagged *PED/PEA-15* cDNA under the control of the CMV promoter. The cells were incubated in the presence of the indicated concentrations of Rtz for 24 h. Total protein extracts were separated by SDS-PAGE and immunoblotted with a specific PED/PEA-15 antibody, which detected both the endogenous (15 kDa) and the exogenous (21 kDa) protein. Results are shown from a representative experiment; qualitatively similar data were obtained in replicate experiments. *B,* transgenic mice overexpressing PED/PEA-15 (Tg_{ped}; $n = 6$), and their nontransgenic littermates (WT; $n = 6$) were treated with 10 mg/kg/die of Rtz for either 3 or 10 days, as indicated. Total protein extracts from gastrocnemius were separated by SDS-PAGE followed by immunoblotting with PED/PEA-15 or 14-3-3ϵ antibody. Blots were revealed by ECL, and autoradiography and the intensity of bands was quantitated by densitometry. *C,* L6 myotubes were transfected with a *PED/PEA-15* cDNA (*dark gray bars*). Both $L6_{wt}$ and $L6_{ped}$ cells were incubated in the absence or presence of 1 μM Rtz for 24 h followed by stimulation with 100 nM insulin (*Ins*) for 30 min. 2-Deoxy-D-glucose (*2-DG*) uptake was assayed as described under "Experimental Procedures." *Bars* represent the means ± S.D. of duplicate (*B*) and triplicate (*C*) determinations in three independent experiments. *Asterisks* denote statistically significant differences (*, $p < 0.05$; **, $p < 0.01$).

regulated the *PED/PEA-15* promoter activity, achieving its maximum effect within 4 h of exposure (Fig. 4*A*). Consistently, a >2-fold increase in *PED/PEA-15* mRNA levels was also demonstrated by quantitative RT-PCR (qRT-PCR) analysis (Fig. 4*B*). Furthermore, TPA effect on both *PED/PEA-15* mRNA levels (Fig. 4*C*) and promoter activity (Fig. 4*D*) was significantly inhibited by treating the cells with Rtz. In addition, the presence

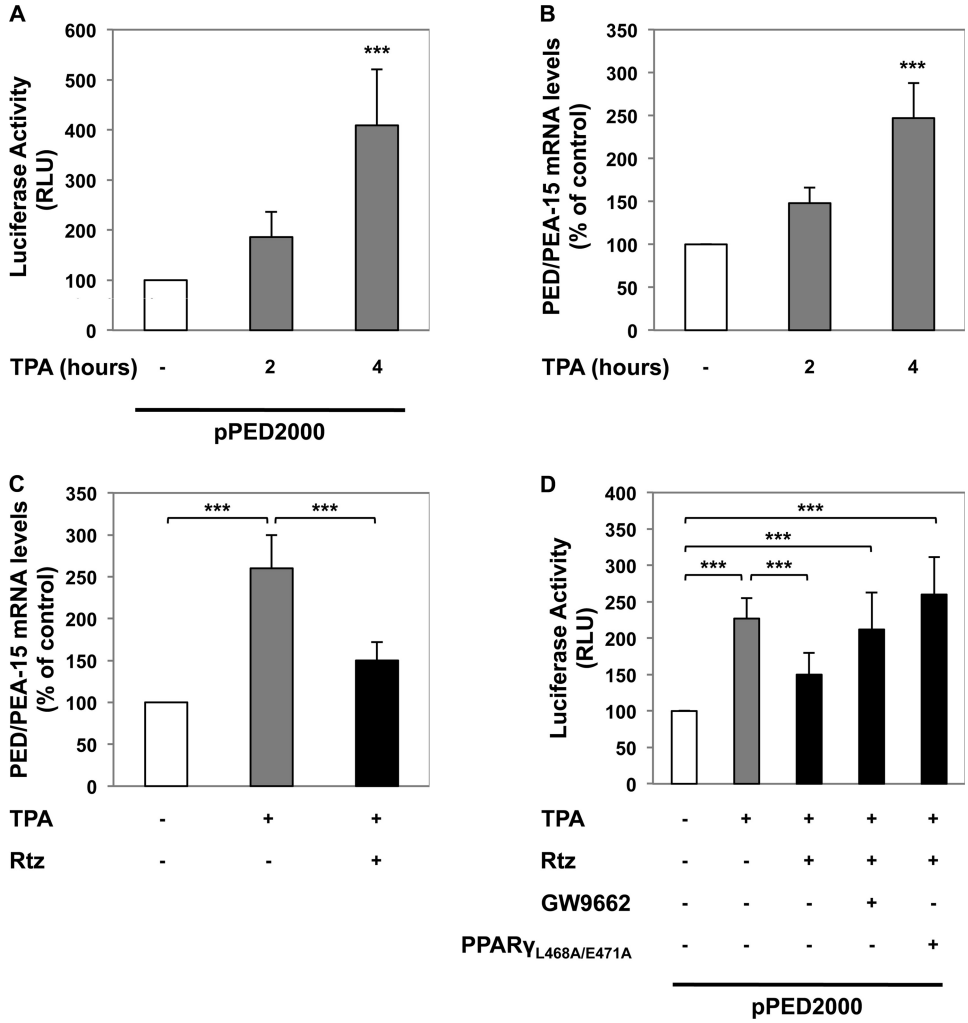

FIGURE 4. **Mechanisms of TPA regulation of *ped/pea-15* promoter activity.** *A* and *D,* HeLa cells, cotransfected with the pPED2000 and pRSV-β-gal constructs, were further transfected with the $PPAR\gamma_{L468A/E471A}$ mutant or pretreated with 10 μM GW9662 for 1 h and subsequently incubated in the absence or presence of 0.1 μM TPA and 1 μM Rtz for 4 h, as indicated. Luciferase activities were measured and normalized for β-galactosidase activities. *Bars* represent the means ± S.D. of four independent experiments each performed in duplicate. *B* and *C,* HeLa cells were incubated in the absence or presence of 0.1 μM TPA and 1 μM Rtz for 4 h, as indicated. *PED/PEA-15* mRNA levels were subsequently quantitated by qRT-PCR, and values were normalized for *GAPDH* of the same samples and shown as fold increase relative to untreated cells. *Bars* represent the means ± S.D. of three independent experiments. *Asterisks* denote statistically significant differences (***, $p < 0.001$).

of the PPARγ antagonist GW9662 as well as that of the dominant negative PPARγ mutant, $PPAR\gamma_{L468A/E471A}$, enabled full TPA effect on promoter activity during simultaneous treatment with Rtz (Fig. 4*D*). These findings initially supported the possibility that PPARγ regulation of *PED/PEA-15* function might involve AP-1 and/or NF-κB transcriptional control.

To further explore this hypothesis, we transfected HeLa cells with either a *PED/PEA-15* deletion construct lacking the NF-κB-binding site but featuring an intact CRE-like site (pPED210) or the same construct where the CRE-like site was mutagenized ($pPED210_{MUT}$). Interestingly, in the former case, exposure to TPA induced a 2.5-fold enhanced transcriptional activity, which was almost completely suppressed by Rtz treatment (Fig. 5*A*). At variance, cells transfected with the CRE-like mutagenized construct exhibited depressed basal promoter activity with complete loss of TPA responsiveness, whether in the absence or presence of Rtz. These observations led us to hypothesize that AP-1 plays a major role in basal and PPARγ-dependent regulation of *PED/PEA-15* expression. Indeed, in cells transfected with the $pPED2000_{MUT}$ construct, which features the intact NF-κB site but the mutated CRE-like site, Rtz treatment failed to repress TPA-induced *PED/PEA-15* promoter activity (Fig. 5*B*), suggesting that NF-κB is not involved in the regulation of *PED/PEA-15* expression by PPARγ.

EMSAs also revealed increased occupancy of the CRE-like site at *PED/PEA-15* promoter in lysates from TPA-treated as compared with untreated HeLa cells (Fig. 6*A*, *left*). This CRE-like site occupancy was dose-dependently inhibited by Rtz. Importantly, supershift assays with a specific c-JUN antibody revealed the presence of the AP-1 component c-JUN in the binding complex at the CRE-like site (Fig. 6*A*, *right*). c-JUN occupancy at the *PED/PEA-15* promoter was also investigated in living cells by ChIP assays. In these experiments, the cross-linked chromatin was precipitated using the c-JUN antibody followed by amplification of the CRE-like site at the human *PED/PEA-15* promoter. As shown in Fig. 6*B*, TPA exposure determined the c-JUN association to the CRE-like site, which was reduced by Rtz treatment in a dose-dependent manner.

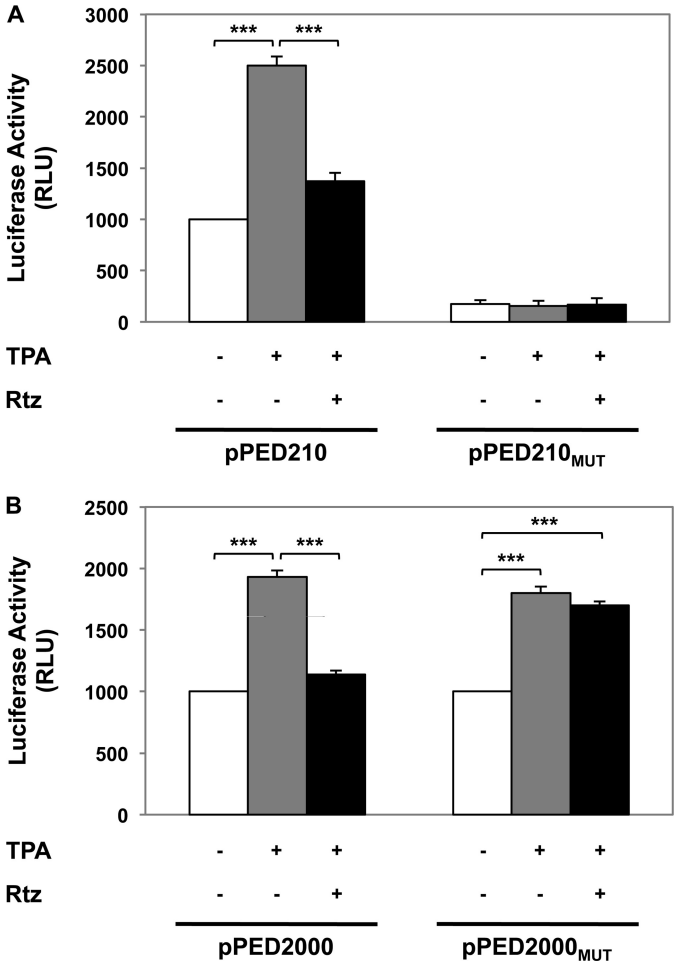

FIGURE 5. **Role of AP-1 in PPARγ-mediated regulation of *ped/pea-15* transcription.** HeLa cells were cotransfected with pPED210 (*A*) or pPED2000 (*B*) or the versions of these constructs featuring the mutagenized CRE-like site ($pPED210_{MUT}$ and $pPED2000_{MUT}$, respectively), in addition to pRSV-β-gal construct. The cells were then incubated in the absence or presence of 0.1 μM TPA and 1 μM Rtz for 4 h. Luciferase activities were normalized to β-galactosidase activities. Data are presented as means ± S.D. of four independent experiments, each in duplicate. *Asterisks* denote statistically significant differences (***, $p < 0.001$).

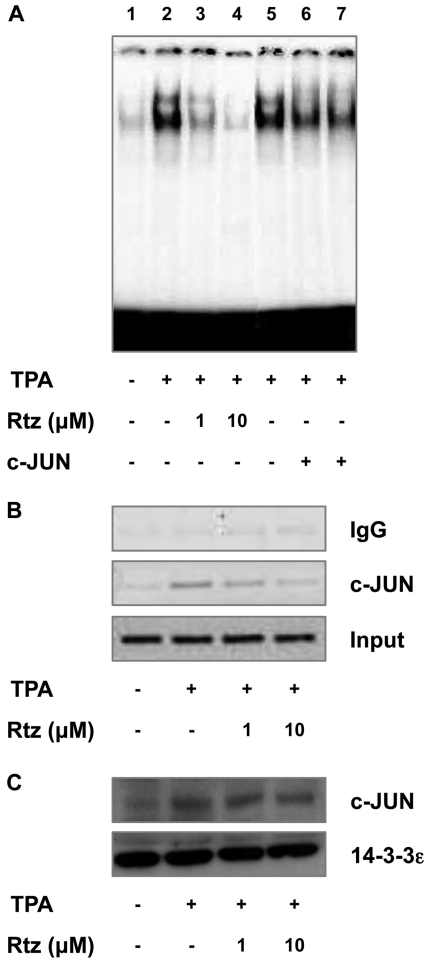

FIGURE 6. **Rtz effect on TPA-induced binding of AP-1 to the CRE-like site at *PED/PEA-15* promoter.** *A,* HeLa cells were incubated in the absence or presence of 0.1 μM TPA and the indicated concentrations of Rtz for 4 h (*lanes 1–4*). Nuclear protein extracts were incubated with a ^{32}P-labeled oligonucleotide encompassing the CRE-like site at *PED/PEA-15* promoter. Nuclear protein extracts from TPA-treated cells were preincubated with c-JUN antibody for different times (1 and 4 h, *lanes 6* and *7*) before adding the radiolabeled probe. The reaction mixtures were separated on 6% nondenaturing polyacrylamide gels, and dried gels were revealed by autoradiography. The autoradiographs shown are representative of four independent experiments. *B,* HeLa cells were incubated in the absence or presence of TPA and Rtz , as indicated; soluble chromatin was prepared and immunoprecipitated with either c-JUN or nonspecific IgG antibody. Chromatin immunoprecipitation was followed by PCR amplification with primers designed for the CRE-like site at the human *PED/PEA-15* promoter. Amplification products were separated on agarose gels and revealed by ethidium bromide. The photograph shown is representative of five independent experiments. *C,* cells were incubated in the absence or presence of TPA and Rtz, as indicated. Total protein extracts were separated by SDS-PAGE, transferred to nitrocellulose filters, and immunoblotted with c-JUN or 14-3-3ε antibody. Blots were revealed by ECL and autoradiography. The autoradiographs shown are representative of three independent experiments.

This effect was not due to a decrease in TPA-induced expression of c-JUN in HeLa cells (Fig. 6*C*).

PPARγ Represses ped/pea-15 Expression via AP-1 in L6 Cells—Based on ChIP assays, Rtz as well as Ptz treatment decreased c-jun binding to the CRE-like site also in L6 myotubes (Fig. 7*A*), confirming the major role of AP-1 in the *ped/pea-15* down-regulation by PPARγ also in skeletal muscle cells. Importantly, in these experiments, the two TZDs did not affect the binding of the NF-κB subunit p65 to its binding site on the *ped/pea-15* promoter (Fig. 7*B*).

In L6 cells, the overexpression of c-JUN (Fig. 8*A*) slightly increased *ped/pea-15* expression in untreated cells (Fig. 8*B*). However, higher levels of ectopic c-JUN bypassed the down-regulation of *ped/pea-15* due to PPARγ (Fig. 8*B*). In parallel, activated PPARγ was not able to displace c-JUN from the CRE-like site at *ped/pea-15* promoter when it was overexpressed in L6 cells (Fig. 8*C*). After c-jun silencing (Fig. 8*A*), L6 cells showed a significantly lower expression of *ped/pea-15* compared with wild-type cells no longer reduced by both Rtz and Ptz (Fig. 8*B*), supporting the major role of AP-1 in *ped/pea-15* down-regulation by PPARγ also in skeletal muscle cells.

PPARγ Decreases ped/pea-15 Expression in High Fat Diet-fed Mice—The *in vivo* significance of *ped/pea-15* regulation by PPARγ agonists was further explored in mice subjected to a high fat diet regimen for 12 weeks. As shown in Table 1, these mice became dyslipidemic and developed significant hyperinsulinemia and insulin resistance. Interestingly, these changes were accompanied by a 2.5-fold increase in *ped/pea-15* expression in their skeletal muscle. Further treatment of these mice

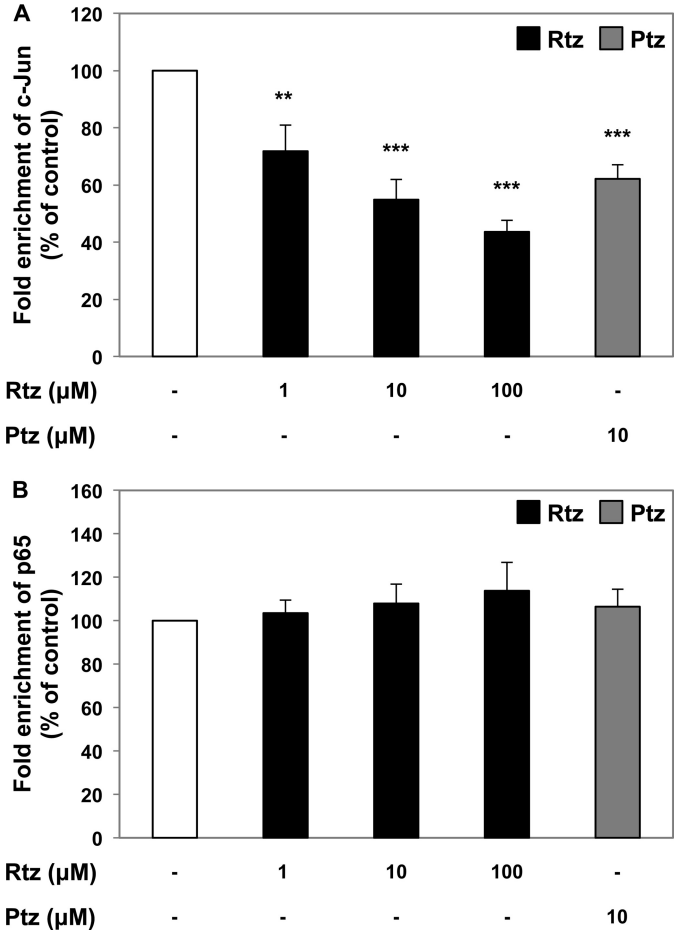

FIGURE 7. **TZD effect on *ped/pea-15* promoter occupancy by c-jun and p65.** L6 myotubes were incubated with either 10 μM Rtz or 10 μM Ptz for 24 h, as indicated. Soluble chromatin was prepared and immunoprecipitated with c-JUN, p65, or nonspecific IgG antibodies. Chromatin immunoprecipitation was followed by PCR amplification with primers designed for either the CRE-like site (*A*) or the NF-κB-binding site (*B*) at the rat *ped/pea-15* promoter. Amplification products were separated by agarose gels and revealed by ethidium bromide. *Bars* represent means ± S.D. of three independent experiments. *Asterisks* denote statistically significant differences (**, $p < 0.01$; ***, $p < 0.001$).

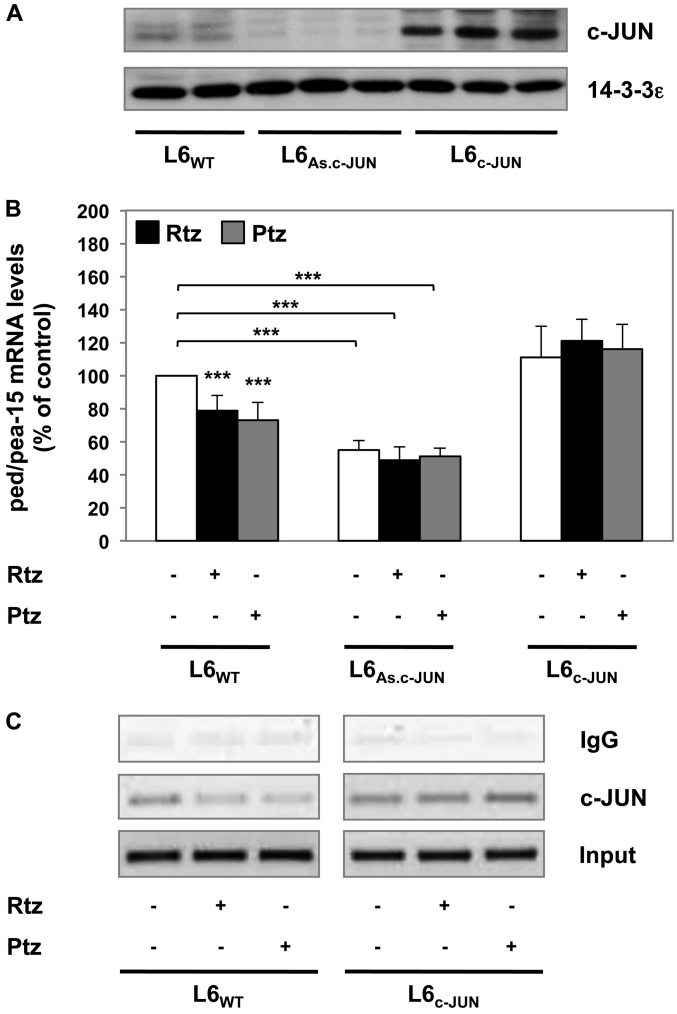

FIGURE 8. **Mechanism of TZD-dependent regulation of *ped/pea-15* expression.** L6 myotubes were transiently transfected with the vector pCEFL containing c-JUN cDNA or c-JUN phosphorothioate antisense oligonucleotides, as indicated. Upon transfection, the cells were incubated with either 10 μM Rtz or 10 μM Ptz for 24 h. *A,* cells were lysed, and total protein extracts were separated by SDS-PAGE followed by immunoblotting with c-JUN or 14-3-3ϵ antibody. Blots were revealed by ECL and autoradiography. *B,* total RNA was obtained, and then *ped/pea-15* and *gapdh* mRNA levels were measured by qRT-PCR. *Bars* represent the means ± S.D. of three independent experiments. *Asterisks* indicate statistically significant differences (*, $p < 0.05$; ***, $p < 0.001$). *C,* L6 myotubes were transiently transfected with the pCEFL containing a c-JUN cDNA before incubating with either 10 μM Rtz or 10 μM Ptz for 24 h. Soluble chromatin was prepared and immunoprecipitated with either c-JUN or nonspecific IgG antibody. Chromatin immunoprecipitation was followed by PCR amplification with primers designed for the CRE-like site at the rat *ped/pea-15* promoter. Amplification products were separated on agarose gels and revealed by ethidium bromide. The photograph shown is representative of three further experiments.

with Rtz for 10 days improved dyslipidemia and plasma insulin levels. Based on the determination of glucose areas under the curves during the accomplishment of insulin tolerance tests, insulin sensitivity was also rescued by Rtz. Simultaneously *ped/pea-15* mRNA levels were significantly reduced, further supporting the important role of *ped/pea-15* in Rtz action *in vivo*.

DISCUSSION

The relevance of adipose tissue *versus* skeletal muscle in mediating PPARγ function in glucose tolerance has been debated (10, 11, 34). PPARγ is a master regulator of adipogenesis (7, 35) whose induction, associated with the capability for fatty acid trapping, has been shown to represent an important contributor to the maintenance of systemic insulin sensitivity (12, 36). However, studies in mice with targeted loss of PPARγ in the skeletal muscle revealed development of severe insulin resistance in these animals (2). Despite development of fat and liver insulin resistance (2, 11), evidence was also obtained that, in these mice, PPARγ directly coordinates glucoregulatory responses in the skeletal muscle and this action is needed for the beneficial effects of PPARγ agonists in ameliorating insulin resistance conditions (10). Comprehensive and unbiased mRNA profiling studies in rats revealed that PPARγ activation has coordinate effects on gene expression in multiple insulin-sensitive tissues, with regulation of specific gene panels in each of these tissues (37).

However, in the skeletal muscle, the panel of the genes regulated by PPARγ is still incomplete, making the molecular details of PPARγ action on muscle glucoregulatory function unclear. In this study, we report that in mouse skeletal muscle tissue and

TABLE 1

Rosiglitazone effects on biochemical parameters of mice subjected to different dietary regimens

All data are presented as means ± S.E. Statistical differences were determined by one- or two-way analysis of variance as appropriate, and Bonferroni post hoc testing was performed when applicable. A p value of <0.05 was considered significant. ITT indicates insulin tolerance test; AUC indicates area under curve; CNV indicates copy number variation; CHOL indicates serum total cholesterol; TG indicates serum triglycerides. Data are means ± S.E. STD indicates standard diet mice; HFD indicates high fat diet mice; HFD+R indicates high fat diet mice after treatment with rosiglitazone 10 mg/kg/10 days, oral gavage.

	STD (n = 10)	HFD (n = 8)	HFD+R (n = 6)
Body weight	28.51 ± 0.99 g	39.11 ± 1.30 g[a]	39.84 ± 2.27 g
Food intake	3.16 ± 0.09 g/mouse/day	2.87 ± 0.2 g/mouse/day	2.40 ± 0.2 g/mouse/day
AUC ITT	9343.5 ± 424.5 mg/dl·120 min	21517.5 ± 1812.7 mg/dl·120 min[a]	14817 ± 1038.5 mg/dl·120 min[b]
PED/PEA-15	2.81 ± 2.1E-05 CNV	6.77 ± 1.23E-04 CNV[b]	5.25 ± 7.75E-05 CNV[c]
CHOL	102.5 ± 6.71 mg/dl	207.33 ± 17.48 mg/dl[b]	130.8 ± 15.73 mg/dl[c]
TG	95.4 ± 6.64 mg/dl	204.23 ± 26.74 mg/dl[b]	83.86 ± 9.97 mg/dl[b]
HDL	47.16 ± 6.70 mg/dl	68.87 ± 11.10 mg/dl	57.74 ± 5.33 mg/dl
LDL	6.25 ± 1.10 mg/dl	15.40 ± 2.30 mg/dl[d]	6.83 ± 0.68 mg/dl[c]
Glucose	107 ± 6.0 mg/dl	180 ± 11 mg/dl[a]	163 ± 6.0 mg/dl[c]
Insulin	0.36 ± 0.13 ng/ml	1.09 ± 0.2 ng/ml[a]	0.68 ± 0.32 ng/ml[c]

[a] Significant differences were between high fat diet mice *versus* standard diet mice and between high fat diet mice after treatment with rosiglitazone *versus* high fat diet mice. $p \leq 0.001$.
[b] $p \leq 0.01$.
[c] Data are indicated by t test.
[d] $p \leq 0.05$.

in L6 skeletal muscle cell line the PPARγ agonists Rtz and Ptz repress the expression of *ped/pea-15*, identifying this gene as a novel downstream target of PPARγ. Indeed, either preincubation with the PPARγ antagonist GW9662 or transfection with the dominant negative PPARγ mutant, $PPAR\gamma_{L468A/E471A}$ (24), completely blocked the Rtz effect.

Previous studies in mice and in humans demonstrated that PED/PEA-15 serves as a physiological regulator of glucose tolerance (13, 38). *PED/PEA-15* is transcriptionally up-regulated in type 2 diabetics as well as in their euglycemic offspring (17), determining insulin resistance in glucose disposal in the skeletal muscle mass (15). The mechanisms of *PED/PEA-15* transcriptional control have been only partially elucidated, but its repression by PPARγ agonists in skeletal muscle may contribute to the beneficial effects of these agents when administered to individuals with abnormalities in glucose tolerance. In support of these conclusions, we observed that, together with its action on *ped/pea-15* transcription, Rtz improved insulin-stimulated glucose uptake in the L6 cells, although both these effects were simultaneously impaired in cells expressing *ped/pea-15* under the control of an exogenous promoter. In addition, the *in vivo* studies reported in this work now show that high fat diet raised the expression of *ped/pea-15* in parallel with the development of insulin resistance, whereas Rtz simultaneously reversed both of these effects.

The finding that *ped/pea-15* is a target of PPARγ prompted us to further explore *in vitro* the details of PPARγ regulation of this gene. Previous studies in cells treated with TPA, a known activator of both AP-1 and NF-κB, revealed increased *ped/pea-15* expression (18), supporting the hypothesis that PPARγ brakes *ped/pea-15* transcription by transrepressing one or both of these transcription factors. Indeed, in the course of this study, we have functionally validated the presence of binding sequences for AP-1 and NF-κB at the promoter of *PED/PEA-15,* and the anti-inflammatory action of PPARγ is known to be mediated to a major extent via transrepression of these factors (39). Interestingly, supershift and ChIP experiments revealed that Rtz reduced *ped/pea-15* promoter occupancy by the c-jun moiety of the AP-1 transcriptional complex. In contrast, NF-κB presence at *ped/pea-15* promoter was unaffected in TZD-treated cells, indicating high specificity in the PPARγ-dependent transcriptional control of *ped/pea-15*. The observation that PPARγ inhibits Jun/AP-1 binding to DNA suggests a potential direct protein-protein interaction between PPARγ and c-Jun. A similar negative interference with AP-1 activity has been described for other nuclear receptors, such as the retinoic acid receptor (40) and the glucocorticoid receptor (41). In these reports, both the glucocorticoid receptor and retinoic acid receptor were shown to form a nonproductive complex with c-jun, leading to a decrease of AP-1 binding activity. Alternatively, PPARγ could block or destabilize an interaction between c-Jun and a cellular factor that facilitates DNA binding. Constructs bearing mutations at the CRE-like site of *PED/PEA-15* promoter, but not within the NF-κB-binding site, failed in affecting promoter activity when AP-1 and NF-κB were activated by TPA. Thus, AP-1 but not NF-κB is necessary for PPARγ control of the *PED/PEA-15* transcription. Furthermore, Rtz treatment in cells upon silencing of c-jun showed no effect on *ped/pea-15* expression, indicating that c-jun transrepression is sufficient for the PPARγ action. The mechanism responsible for the Rtz effect on *ped/pea-15* promoter occupancy by c-jun was not based on changes in the levels of c-jun itself. Alternatively, Rtz might impair ability of c-jun to bind to the *ped/pea-15* promoter, as forcing its occupancy by c-jun overexpression blocked the Rtz repression of *ped/pea-15*.

The chronic low grade inflammation induced by obesity is well recognized as a key trait of type 2 diabetes (42), as a number of inflammatory pathways are activated in classical insulin target tissues of these individuals (43, 44). These signaling cascades include the JNK/AP-1 network that is known to be down-regulated by PPARγ (39). However, genes that are ultimately involved in the impairment of glucose tolerance induced by inflammatory stimuli are still largely unknown. We now report that *ped/pea-15* expression is controlled by physiological levels of c-jun in the cells. Indeed, c-jun silencing with specific antisense impairs basal *ped/pea-15* expression. In addition, PPARγ activating anti-inflammatory agents regulate *ped/pea-15* by reducing c-jun occupancy at its promoter. These findings identify *ped/pea-15* as a gene whose transcription may change in response to common abnormalities typical of the low grade

unresolved inflammation associated with type 2 diabetes. Further studies assessing *ped/pea-15* function may offer previously unrecognized opportunities to identify these abnormalities.

Acknowledgments—We thank Dr. Mitchell Lazar (University of Pennsylvania, Philadelphia) for kindly providing the PPRE3-tk-luciferase construct. The dominant negative PPARγ expression vector was kindly provided by Dr. V. K. K. Chatterjee (University of Cambridge, Cambridge, UK). We also thank to Dr. Domenico Liguoro for helpful advice with cell culture technologies.

REFERENCES

1. Gurnell, M., and Chatterjee, V. K. (2004) Nuclear receptors in disease. Thyroid receptor β, peroxisome proliferator-activated receptor γ, and orphan receptors. *Essays Biochem.* **40,** 169–189
2. Kintscher, U., and Law, R. E. (2005) PPARγ-mediated insulin sensitization. The importance of fat *versus* muscle. *Am. J. Physiol. Endocrinol. Metab.* **288,** E287–E291
3. Rosen, E. D., and Spiegelman, B. M. (2001) PPARγ. A nuclear regulator of metabolism, differentiation, and cell growth. *J. Biol. Chem.* **276,** 37731–37734
4. Tontonoz, P., and Spiegelman, B. M. (2008) Fat and beyond: the diverse biology of PPARγ. *Annu. Rev. Biochem.* **77,** 289–312
5. Donath, M. Y., and Shoelson, S. E. (2011) Type 2 diabetes as an inflammatory disease. *Nat. Rev. Immunol.* **11,** 98–107
6. Frias, J. P., Yu, J. G., Kruszynska, Y. T., and Olefsky, J. M. (2000) Metabolic effects of troglitazone therapy in type 2 diabetic, obese, and lean normal subjects. *Diabetes Care* **23,** 64–69
7. Miyazaki, Y., Mahankali, A., Matsuda, M., Glass, L., Mahankali, S., Ferrannini, E., Cusi, K., Mandarino, L. J., and DeFronzo, R. A. (2001) Improved glycemic control and enhanced insulin sensitivity in type 2 diabetic subjects treated with pioglitazone. *Diabetes Care* **24,** 710–719
8. Nolan, J. J., Ludvik, B., Beerdsen, P., Joyce, M., and Olefsky, J. (1994) Improvement in glucose tolerance and insulin resistance in obese subjects treated with troglitazone. *N. Engl. J. Med.* **331,** 1188–1193
9. Raskin, P., Rappaport, E. B., Cole, S. T., Yan, Y., Patwardhan, R., and Freed, M. I. (2000) Rosiglitazone short-term monotherapy lowers fasting and post-prandial glucose in patients with type II diabetes. *Diabetologia* **43,** 278–284
10. Hevener, A. L., He, W., Barak, Y., Le, J., Bandyopadhyay, G., Olson, P., Wilkes, J., Evans, R. M., and Olefsky, J. (2003) Muscle-specific Pparγ deletion causes insulin resistance. *Nat. Med.* **9,** 1491–1497
11. Norris, A. W., Chen, L., Fisher, S. J., Szanto, I., Ristow, M., Jozsi, A. C., Hirshman, M. F., Rosen, E. D., Goodyear, L. J., Gonzalez, F. J., Spiegelman, B. M., and Kahn, C. R. (2003) Muscle-specific PPARγ-deficient mice develop increased adiposity and insulin resistance but respond to thiazolidinediones. *J. Clin. Invest.* **112,** 608–618
12. Shulman, G. I. (2000) Cellular mechanisms of insulin resistance. *J. Clin. Invest.* **106,** 171–176
13. Condorelli, G., Vigliotta, G., Iavarone, C., Caruso, M., Tocchetti, C. G., Andreozzi, F., Cafieri, A., Tecce, M. F., Formisano, P., Beguinot, L., and Beguinot, F. (1998) PED/PEA-15 gene controls glucose transport and is overexpressed in type 2 diabetes mellitus. *EMBO J.* **17,** 3858–3866
14. Fiory, F., Formisano, P., Perruolo, G., and Beguinot, F. (2009) Frontiers. PED/PEA-15, a multifunctional protein controlling cell survival and glucose metabolism. *Am. J. Physiol. Endocrinol. Metab.* **297,** E592–E601
15. Condorelli, G., Vigliotta, G., Trencia, A., Maitan, M. A., Caruso, M., Miele, C., Oriente, F., Santopietro, S., Formisano, P., and Beguinot, F. (2001) Protein kinase C (PKC)-α activation inhibits PKC-ζ and mediates the action of PED/PEA-15 on glucose transport in the L6 skeletal muscle cells. *Diabetes* **50,** 1244–1252
16. Viparelli, F., Cassese, A., Doti, N., Paturzo, F., Marasco, D., Dathan, N. A., Monti, S. M., Basile, G., Ungaro, P., Sabatella, M., Miele, C., Teperino, R., Consiglio, E., Pedone, C., Beguinot, F., Formisano, P., and Ruvo, M. (2008) Targeting of PED/PEA-15 molecular interaction with phospholipase D1 enhances insulin sensitivity in skeletal muscle cells. *J. Biol. Chem.* **283,** 21769–21778
17. Valentino, R., Lupoli, G. A., Raciti, G. A., Oriente, F., Farinaro, E., Della Valle, E., Salomone, M., Riccardi, G., Vaccaro, O., Donnarumma, G., Sesti, G., Hribal, M. L., Cardellini, M., Miele, C., Formisano, P., and Beguinot, F. (2006) The PEA15 gene is overexpressed and related to insulin resistance in healthy first-degree relatives of patients with type 2 diabetes. *Diabetologia* **49,** 3058–3066
18. Perfetti, A., Oriente, F., Iovino, S., Alberobello, A. T., Barbagallo, A. P., Esposito, I., Fiory, F., Teperino, R., Ungaro, P., Miele, C., Formisano, P., and Beguinot, F. (2007) Phorbol esters induce intracellular accumulation of the anti-apoptotic protein PED/PEA-15 by preventing ubiquitinylation and proteasomal degradation. *J. Biol. Chem.* **282,** 8648–8657
19. Ungaro, P., Teperino, R., Mirra, P., Longo, M., Ciccarelli, M., Raciti, G. A., Nigro, C., Miele, C., Formisano, P., and Beguinot, F. (2010) Hepatocyte nuclear factor (HNF)-4α-driven epigenetic silencing of the human PED gene. *Diabetologia* **53,** 1482–1492
20. Schlingensiepen, K. H., Schlingensiepen, R., Kunst, M., Klinger, I., Gerdes, W., Seifert, W., and Brysch, W. (1993) Opposite functions of jun-B and c-jun in growth regulation and neuronal differentiation. *Dev. Genet.* **14,** 305–312
21. Ungaro, P., Teperino, R., Mirra, P., Cassese, A., Fiory, F., Perruolo, G., Miele, C., Laakso, M., Formisano, P., and Beguinot, F. (2008) Molecular cloning and characterization of the human PED/PEA-15 gene promoter reveal antagonistic regulation by hepatocyte nuclear factor 4α and chicken ovalbumin upstream promoter transcription factor II. *J. Biol. Chem.* **283,** 30970–30979
22. Condorelli, G., Trencia, A., Vigliotta, G., Perfetti, A., Goglia, U., Cassese, A., Musti, A. M., Miele, C., Santopietro, S., Formisano, P., and Beguinot, F. (2002) Multiple members of the mitogen-activated protein kinase family are necessary for PED/PEA-15 anti-apoptotic function. *J. Biol. Chem.* **277,** 11013–11018
23. DuBois, R. N., Gupta, R., Brockman, J., Reddy, B. S., Krakow, S. L., and Lazar, M. A. (1998) The nuclear eicosanoid receptor, PPARγ, is aberrantly expressed in colonic cancers. *Carcinogenesis* **19,** 49–53
24. Gurnell, M., Wentworth, J. M., Agostini, M., Adams, M., Collingwood, T. N., Provenzano, C., Browne, P. O., Rajanayagam, O., Burris, T. P., Schwabe, J. W., Lazar, M. A., and Chatterjee, V. K. (2000) A dominant-negative peroxisome proliferator-activated receptor γ (PPARγ) mutant is a constitutive repressor and inhibits PPARγ-mediated adipogenesis. *J. Biol. Chem.* **275,** 5754–5759
25. Tremblay, F., and Marette, A. (2001) Amino acid and insulin signaling via the mTOR/p70 S6 kinase pathway. A negative feedback mechanism leading to insulin resistance in skeletal muscle cells. *J. Biol. Chem.* **276,** 38052–38060
26. Wheatley, K. E., Nogueira, L. M., Perkins, S. N., and Hursting, S. D. (2011) Differential effects of calorie restriction and exercise on the adipose transcriptome in diet-induced obese mice. *J. Obes.* **2011,** 265417
27. Miele, C., Raciti, G. A., Cassese, A., Romano, C., Giacco, F., Oriente, F., Paturzo, F., Andreozzi, F., Zabatta, A., Troncone, G., Bosch, F., Pujol, A., Chneiweiss, H., Formisano, P., and Beguinot, F. (2007) PED/PEA-15 regulates glucose-induced insulin secretion by restraining potassium channel expression in pancreatic beta-cells. *Diabetes* **56,** 622–633
28. Bradford, M. M. (1976) A rapid and sensitive method for the quantitation of microgram quantities of protein utilizing the principle of protein-dye binding. *Anal. Biochem.* **72,** 248–254
29. Livak, K. J., and Schmittgen, T. D. (2001) Analysis of relative gene expression data using real time quantitative PCR and the $2(-\Delta\Delta C(T))$ Method. *Methods* **25,** 402–408
30. Whelan, J. A., Russell, N. B., and Whelan, M. A. (2003) A method for the absolute quantification of cDNA using real time PCR. *J. Immunol. Methods* **278,** 261–269
31. Dignam, J. D., Lebovitz, R. M., and Roeder, R. G. (1983) Accurate transcription initiation by RNA polymerase II in a soluble extract from isolated mammalian nuclei. *Nucleic Acids Res.* **11,** 1475–1489
32. Ricote, M., and Glass, C. (2007) PPARs and molecular mechanism of transrepression. *Biochim. Biophys. Acta* **1771,** 926–935
33. Medcalf, R. L., Rüegg, M., and Schleuning, W. D. (1990) A DNA motif

related to the cAMP-responsive element and an exon-located activator protein-2-binding site in the human tissue-type plasminogen activator gene promoter cooperate in basal expression and convey activation by phorbol ester and cAMP. *J. Biol. Chem.* **265,** 14618–14626
34. Zierath, J. R., Ryder, J. W., Doebber, T., Woods, J., Wu, M., Ventre, J., Li, Z., McCrary, C., Berger, J., Zhang, B., and Moller, D. E. (1998) Role of skeletal muscle in thiazolidinedione insulin sensitizer (PPARγ agonist) action. *Endocrinology* **139,** 5034–5041
35. Kubota, N., Terauchi, Y., Miki, H., Tamemoto, H., Yamauchi, T., Komeda, K., Satoh, S., Nakano, R., Ishii, C., Sugiyama, T., Eto, K., Tsubamoto, Y., Okuno, A., Murakami, K., Sekihara, H., Hasegawa, G., Naito, M., Toyoshima, Y., Tanaka, S., Shiota, K., Kitamura, T., Fujita, T., Ezaki, O., Aizawa, S., Kadowaki, T., *et al.* (1999) PPARγ mediates high fat diet-induced adipocyte hypertrophy and insulin resistance. *Mol. Cell* **4,** 597–609
36. Samuel, V. T., and Shulman, G. I. (2012) Mechanisms for insulin resistance: common threads and missing links. *Cell* **148,** 852–871
37. Way, J. M., Harrington, W. W., Brown, K. K., Gottschalk, W. K., Sundseth, S. S., Mansfield, T. A., Ramachandran, R. K., Willson, T. M., and Kliewer, S. A. (2001) Comprehensive messenger ribonucleic acid profiling reveals that peroxisome proliferator-activated receptor γ activation has coordinate effects on gene expression in multiple insulin-sensitive tissues. *Endocrinology* **142,** 1269–1277
38. Vigliotta, G., Miele, C., Santopietro, S., Portella, G., Perfetti, A., Maitan, M. A., Cassese, A., Oriente, F., Trencia, A., Fiory, F., Romano, C., Tiveron, C., Tatangelo, L., Troncone, G., Formisano, P., and Beguinot, F. (2004) Overexpression of the *ped/pea-15* gene causes diabetes by impairing glucose-stimulated insulin secretion in addition to insulin action. *Mol. Cell. Biol.* **24,** 5005–5015
39. Blanquart, C., Barbier, O., Fruchart, J. C., Staels, B., and Glineur, C. (2003) Peroxisome proliferator-activated receptors. Regulation of transcriptional activities and roles in inflammation. *J. Steroid Biochem. Mol. Biol.* **85,** 267–273
40. Schüle, R., Rangarajan, P., Yang, N., Kliewer, S., Ransone, L. J., Bolado, J., Verma, I. M., and Evans, R. M. (1991) Retinoic acid is a negative regulator of AP-1 responsive genes. *Proc. Natl. Acad. Sci. U.S.A.* **88,** 6092–6096
41. Jonat, C., Rahmsdorf, H. J., Park, K. K., Cato, A. C., Gebel, S., Ponta, H., and Herrlich, P. (1990) Antitumor promotion and anti-inflammation. Down-modulation of AP-1 (Fos/jun) activity by glucocorticoid hormone. *Cell* **62,** 1189–1204
42. Osborn, O., and Olefsky, J. M. (2012) The cellular and signaling networks linking the immune system and metabolism in disease. *Nat. Med.* **18,** 363–374
43. Itani, S. I., Ruderman, N. B., Schmieder, F., and Boden, G. (2002) Lipid-induced insulin resistance in human muscle is associated with changes in diacylglycerol, protein kinase C, and IκB-α. *Diabetes* **51,** 2005–2011
44. Bandyopadhyay, G. K., Yu, J. G., Ofrecio, J., and Olefsky, J. M. (2005) Increased p85/55/50 expression and decreased phosphatidylinositol 3-kinase activity in insulin-resistant human skeletal muscle. *Diabetes* **54,** 2351–2359